

DOI: 10.1002/((please add manuscript number))

**Article type: Communication**

**Room-Temperature Plasma-Assisted Inkjet Printing of Highly Conductive Silver on Paper**

*Caroline E. Knapp,\* Jean-Baptiste Chemin, Samuel P. Douglas, Dominique Abessolo Ondo, Jérôme Guillot, Patrick Choquet, Nicolas D. Boscher\**

Dr. C. E. Knapp, S. P. Douglas

Department of Chemistry

University College London

20 Gordon Street, London, WC1H 0AJ, UK

E-mail: [Caroline.knapp@ucl.ac.uk](mailto:Caroline.knapp@ucl.ac.uk)

J.-B. Chemin, D. Abessolo Ondo, Dr. J. Guillot, Dr. P. Choquet, Dr. N. D. Boscher

Department of Materials Research and Technology

Luxembourg Institute of Science and Technology

5 Avenue des Hauts-Fourneaux, Esch/Alzette, L-4362, Luxembourg

E-mail: [Nicolas.boscher@list.lu](mailto:Nicolas.boscher@list.lu)

Keywords: silver patterning, MOD inks, room-temperature, inkjet printing, atmospheric plasma

Paper, which is a cheap renewable, lightweight and flexible material,<sup>[1]</sup> is foreseen as an essential component in the elaboration of a new generation of recyclable electronic devices such as smart labels or packages, paper displays and disposable sensors.<sup>[2]</sup> The formation of highly conductive features on paper is decidedly desirable for the preparation of paper-based electronic devices<sup>[3]</sup> and for at least a decade, printing has presented itself as an attractive technique to meet the challenges that development poses.<sup>[4,5]</sup> Printed electronics are already used in a range of applications including photovoltaics, antennae, radio frequency identification (RFID) tags,<sup>[6]</sup> as well as in displays<sup>[7]</sup> and sensors.<sup>[8,9]</sup> Arguably printings' biggest boast is its adaptability to

various substrates, as different types of printing are able to deposit conductive metal tracks onto a range of substrates, including paper.<sup>[1]</sup> Presently most commercially used inks in the printed electronics market contain nanoparticles (NPs),<sup>[10,11]</sup> and most are silver based due to its excellent conductivity (*i.e.*  $6.3 \times 10^7 \text{ S m}^{-1}$ ),<sup>[12]</sup> and high standard electrode potential, resulting in a lower sensitivity to oxidation. Direct printing of NP-based conductive inks onto paper substrates has encountered difficulties as the NPs are prone to penetrate into the pores of the paper and become partially segmented.<sup>[1,13]</sup>

Precursors, as opposed to NPs are typically formulated into inks where additives can be used for example to stabilise, aid wetting or control viscosity; and are viewed as an emerging alternative.<sup>[14]</sup> These precursors containing the required metal are typically oxidised and bound with ligands, such that upon specific treatment, the metal centre is reduced and the ligands decompose cleanly, leaving conductive metal features. Silver(I) is the most common oxidation state of silver and it is exclusively used in silver metal deposition, in both chemical vapour deposition (CVD) and ink deposition.<sup>[14]</sup> Most organo-silver complexes synthesised for silver metal deposition are based on silver-oxygen bonds, such as carboxylates<sup>[15]</sup> and diketonates.<sup>[16]</sup> Compounds with silver-nitrogen bonds are becoming increasingly prevalent,<sup>[17]</sup> in particular precursors synthesised from silver nitrate as a starting material. Nevertheless, aqueous silver nitrate inks are light sensitive and require high decomposition temperatures, typically 440 °C, and hence are not particularly useful for paper electronics.<sup>[15]</sup> Recently, Walker *et al.* reported the formulation of precursor inks combining aqueous ammonium hydroxide with silver acetate and formic acid to produce highly conductive features (*ca.*  $10^6 \text{ S cm}$ ) when dried at room-temperature for 24 hours.<sup>[5]</sup> Despite the long drying time of 24 hours, this was an impressive benchmark result and outperformed by far any NPs inks dried at room-temperature.<sup>[5]</sup> However, such an approach is inefficient on paper due to the fast wetting, penetration and decomposition of the ink into porous substrates.<sup>[1]</sup>

Walker *et al.* demonstrated that thermal sintering at 90 °C of their ink led to a significant decrease of the processing time (*i.e.* 15 minutes), while promoting the formation of silver layers with an electrical conductivity identical to that of bulk silver.<sup>[5]</sup> Following this result, several other metal-organic decomposition (MOD) inks have been investigated,<sup>[17]</sup> particularly with the perspective to develop increasingly stable inks which have a suitable viscosity facilitating easier deposition and lower temperature conversion to metal. In addition, whether the ink be NPs-based or a MOD precursor formulation, efforts have been made to reduce the processing time and temperature,<sup>[18]</sup> which is an equally important variable to consider when targeting paper substrates.<sup>[1]</sup> Several alternatives to thermal sintering, which is too time consuming to be easily incorporated into industrial processes, have been proposed.<sup>[6]</sup> Notably, the ink reported by Walker *et al.* was used to produce highly conductive (*i.e.*  $4.8 \times 10^7 \text{ S m}^{-1}$ ) features of silver on polyimide using a continuous wave laser direct synthesis and patterning process.<sup>[19]</sup> UV light and intense pulsed visible light have also been reported to ensure the room-temperature sintering of both MOD inks<sup>[20]</sup> and silver NPs<sup>[21]</sup> on polymer substrates and form highly conductive silver coatings on polymer foils. The multistep electrical sintering of silver NPs was also demonstrated to form highly conductive (*i.e.*  $4.8 \times 10^7 \text{ S m}^{-1}$ ) silver layers on resin-coated photobase paper.<sup>[22]</sup> Furthermore, the microwave sintering of MOD inks has also been investigated, with one of the limiting factors being the 1.3  $\mu\text{m}$  penetration depth of the 2.54 GHz radiation in silver.<sup>[23]</sup> In addition, it was noted that microwave sintering for longer than 1 s at a power of 1 W was shown to cause damage to the plastic substrate through the heat dissipation from the metal layer.<sup>[24]</sup>

In many chemical reactions, plasmas provide an alternative to thermal heating, allowing the deposition of a wide range of materials at much lower substrate temperature than conventional CVD.<sup>[25]</sup> The most common examples being the atmospheric-plasma-enhanced (AP-PE)CVD

of SiO<sub>2</sub> thin films at room-temperature<sup>[26]</sup> or the significantly lower temperatures observed for the AP-PECVD of anatase TiO<sub>2</sub> layers.<sup>[27]</sup> In recent times, several groups have proposed the use of low-pressure plasmas to produce conductive silver on polymer or glass substrates from NPs<sup>[11,28]</sup> and MOD inks.<sup>[29]</sup> The low-pressure plasma approach has even been adapted for the preparation of silver layers on silicone-coated paper.<sup>[6]</sup> However, a 5 minutes drying step at 100 °C was introduced to lower the resistance of the silver coating. Exploiting the reactivity of MOD inks and the potential of atmospheric-pressure plasmas, we have explored for the first time the atmospheric-pressure and room-temperature plasma-assisted inkjet printing of MOD inks on paper, which result in the formation of highly conductive (*i.e.*  $3.8 \times 10^6 \text{ S m}^{-1}$ ) silver lines on uncoated paper. In contrast to the previously described approaches, the silver layers were promptly formed from an up-scalable, substrate independent and versatile method, overcoming the wetting issues often encountered on porous substrates such as paper.

To illustrate our approach, an aqueous silver complex MOD ink (*i.e.*  $[\text{Ag}(\text{NH}_3)_2]^+[\text{C}_2\text{H}_3\text{O}_2]^-$ , Figure S1), whose synthesis is reported in the literature,<sup>[5]</sup> was selected. In contrast to the previously reported silver patterns made from MOD inks, the sintering step was achieved at room-temperature and atmospheric-pressure thanks to an argon-hydrogen plasma generated in a dielectric barrier discharge reactor (DBD). The MOD ink was inkjet printed on paper using an ultrasonic nozzle (Figure 1b, step i). To ensure an efficient plasma sintering of the MOD ink, as well as prevent any detrimental wetting and absorption on the paper substrates, small amounts of the MOD ink were deposited per cycle (*ca.*  $14 \text{ nL cm}^{-2}$ ). In addition, high processing speeds were employed (*i.e.*  $10 \text{ cm s}^{-1}$ ), reducing the delay between the inkjet printing step and the plasma sintering step (*ca.*  $800 \mu\text{s}$ ), in order to prevent the evaporation of the MOD ink components, which would cause decomposition into a brownish coating that cannot be further reduced to metallic silver. The plasma sintering step was performed using a DBD supplied with an argon-hydrogen mixture and ignited using a 10,000 Hz high-voltage

alternating current (Figure 1b, step ii). The argon-hydrogen plasma gas composition was set to 97.5 %-2.5 %, allowing to maximise the concentration of reactive hydrogen species,<sup>[30]</sup> which contribute to the low-temperature reduction of the MOD ink<sup>[31]</sup> and promote a non-thermal desorption of the ligands (Figure 1b, step ii).<sup>[32]</sup> The rather low power dissipated in the plasma discharge (*ca.* 2 W cm<sup>-2</sup>) and the short plasma exposure time (*ca.* 2 s per cycle) allowed the substrate to stay at room-temperature at all times, such as evidenced by means of a thermocouple placed under the paper substrate on the moving stage.

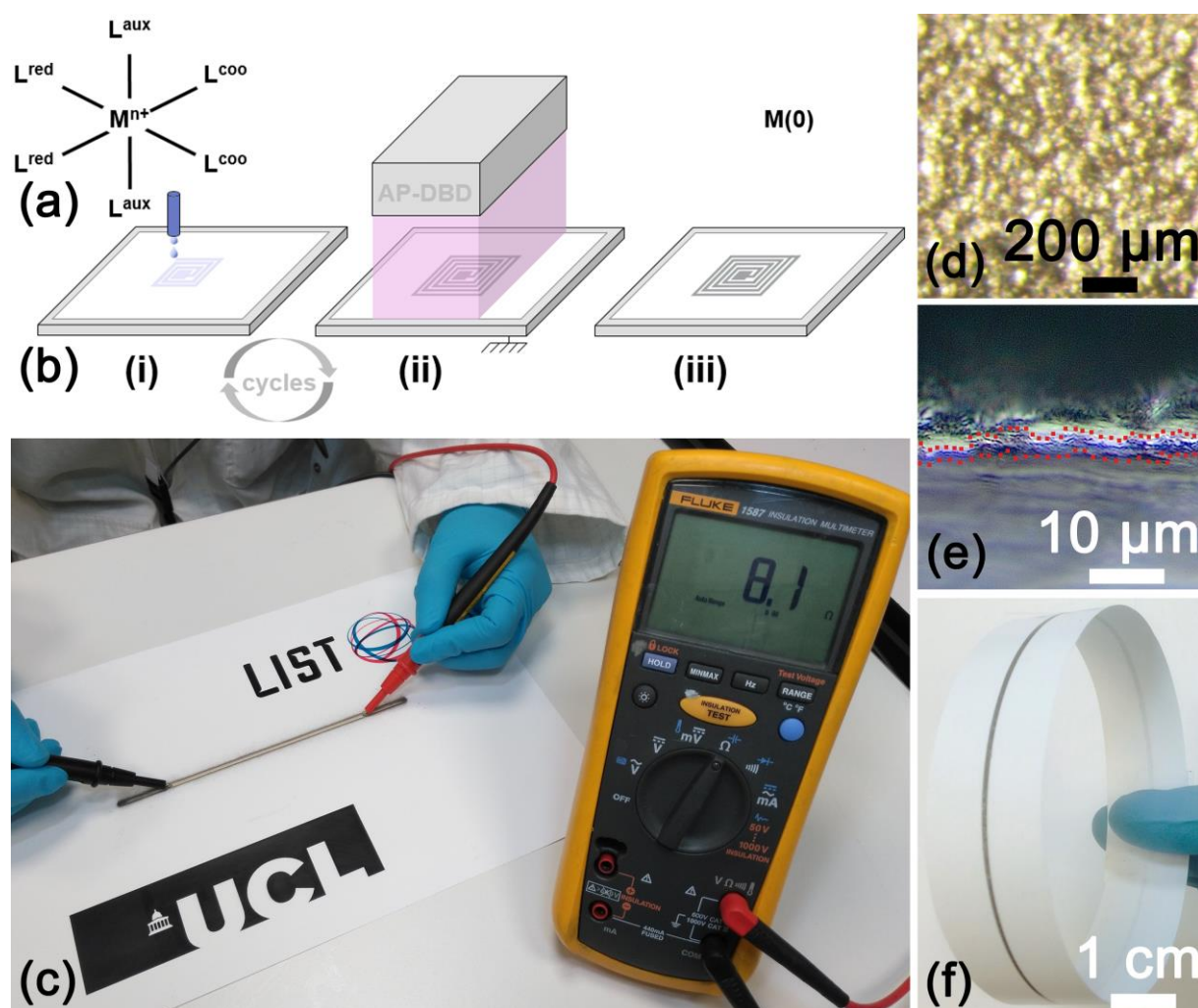


**Figure 1.** Plasma-assisted inkjet printing of highly conductive silver on paper. a) Generic example of a MOD complex where ‘n<sup>+</sup>’ indicates the charge on the metal, ligands are denoted as ‘L’ and are sub-divided into the types: ‘coo’ for coordination, ‘red’ for reduction and ‘aux’ for auxiliary stabilising ligands. b) Schematic of the plasma-assisted inkjet printing process: (i) the MOD ink is deposited onto the substrate, (ii) which is subsequently briefly exposed to an

AP-DBD generated in argon-hydrogen (iii) to form highly conductive silver patterns. c) Photograph of a plasma-assisted inkjet printed silver line on paper. The multimeter reading shown is  $8.1 \Omega$  across a length of approximately 12 cm. d) Top down high magnification microscope image of plasma-assisted inkjet printed silver on paper. e) Cross-sectional microscope image showing a  $2 \mu\text{m}$  thick plasma-assisted inkjet printed silver line on paper and f) front and back-side large area plasma-assisted inkjet printed silver line on folded paper substrate.

The inkjet printing and plasma sintering steps were repeated to ensure the continuous coverage of the rough paper substrate ( $S_a = 94 \text{ nm}$ ). As a result of the plasma-assisted inkjet printing procedure described, lines measuring  $2 \mu\text{m}$  in thickness with low resistivity were formed on paper (Figure 1c). The coatings, with a silvery metallic aspect, continuously covered the paper substrate such as observed by optical microscopy (Figure 1d). Furthermore, in spite of the porous nature of the paper substrate, the backside of the paper is shown evidencing that the MOD ink does not saturate the paper substrate (Figure 1f). This is likely due to the speed of the chemical conversion from MOD ink to conductive silver *via* the plasma. Probing this further, optical microscopy was used to gauge the extent of permeation of the ink into the paper substrate. The cross-sectional observations of the silver deposits on paper indicate permeation depth of the MOD ink to be negligible (Figure 1e).

In contrast to the silvery metallic aspect of the highly conductive plasma-assisted inkjet printed line on paper shown in Figures 1c & d, the room-temperature drying of the MOD ink on paper led to the formation of a brownish film. This is unsurprising since the decomposition of the MOD ink under thermal conditions only begins *ca.*  $80 \text{ }^\circ\text{C}$  and continues in one single step until just after  $140 \text{ }^\circ\text{C}$  where upon it is completely converted to silver metal (Figure 2a). Both the TGA and DSC curves evidence a continuous thermal decomposition and an overall mass loss

of 78 %. Such observations are consistent with previous reports where the MOD ink was held at 90 °C for 15 minutes to ensure its complete conversion to silver metal.<sup>[5]</sup>

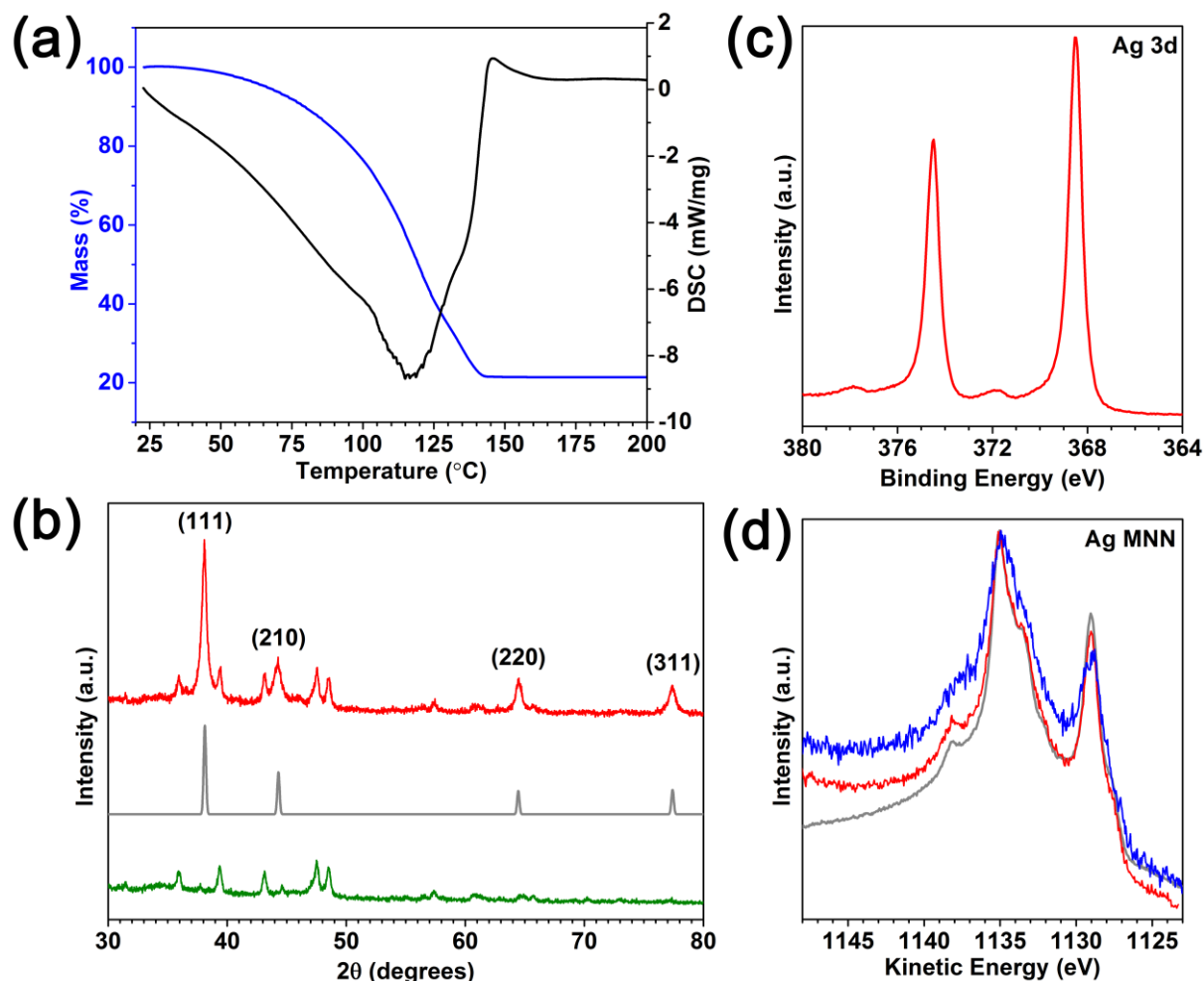


**Figure 2.** Room-temperature conversion of the MOD ink to metallic silver. a) Thermal gravimetric analysis (TGA) (blue) and difference scanning calorimetry (DSC) (black) of the MOD ink from 0 – 200 °C. b) Indexed XRD pattern of plasma-assisted inkjet printed silver on paper over the range of  $30^\circ < 2\theta < 80^\circ$  (red), standard patterns for bulk silver (grey) and the paper substrate (green) are given for comparison. c) XPS spectra showing the Ag 3d transitions for silver on paper. d) XPS spectra showing the Ag MNN Auger transitions for: silver printed on paper (red), silver oxide formed from the decomposition of the ink on paper (blue) and a comparison with pure bulk reference metallic silver (grey).

X-ray diffraction (XRD) analysis of the plasma-assisted inkjet printed line on paper indicates the formation of silver. Bragg peaks at  $38.1^\circ$ ,  $44.3^\circ$ ,  $64.5^\circ$  and  $77.4^\circ$   $2\theta$  match the (111), (210),

(220) and (311) for silver crystallized in the cubic space group  $Fm\bar{3}m$  (Figure 2b). All other features in the pattern were assigned to the paper substrate (Figure 2b). In contrast to the drop-cast films produced from the same MOD ink dried at 23 °C for 24 hours,<sup>[5]</sup> no silver acetate peaks were observed for the plasma-assisted inkjet printed silver line produced at room-temperature.

X-ray photoelectron spectroscopy (XPS) analysis of the plasma-assisted inkjet printed silver on paper revealed peaks at 368.5 and 374.5 eV corresponding to the 3d<sub>5/2</sub> and 3d<sub>3/2</sub> peaks of Ag, respectively (Figure 2c). The positions of the Ag 3d spin-orbit components, separated by *ca.* 6 eV, and the presence of loss features at their higher binding energy side is consistent with formation of metallic silver.<sup>[33]</sup> XPS and energy-dispersive X-ray spectroscopy (EDX) also revealed a high relative weight concentration of Ag (*ca.* 91 wt % and 99 wt %, respectively) in the plasma-assisted inkjet printed silver on paper. This contrasts with the initial Ag weight concentration of the MOD ink (*ca.* 22 wt %) and confirms the interest of the proposed approach with XPS and EDX revealing the relative weight concentration of C and O down to 4 and 1 wt % and 5 and 0 wt % after plasma sintering, respectively. As a comparison, Walker *et al.* reported that the room-temperature decomposition of the MOD ink led to coatings composed of *ca.* 57 wt % silver and 43 wt % silver acetate.<sup>[5]</sup> To undoubtedly confirm the oxidation state of the plasma-assisted inkjet printed silver on paper, the shape of the Ag MNN Auger transition is compared with a pure bulk silver reference in Figure 2d. To negate the possible issue of charge effects and to also confirm the silver oxidation state, the Auger parameters have also been calculated. For the plasma-assisted inkjet printed silver on paper:  $\alpha$  (Ag 3d – Ag M<sub>5</sub>N<sub>4,5</sub>N<sub>4,5</sub>) = 720 eV and  $\alpha$  (Ag 3d – Ag M<sub>4</sub>N<sub>4,5</sub>N<sub>4,5</sub>) = 726.1 eV, which is consistent with literature values for silver metal, *i.e.* Ag(0).<sup>[34]</sup> Furthermore, the Auger parameters calculated for the decomposition of the MOD ink on paper at room-temperature (without plasma treatment) are  $\alpha$  (Ag 3d – Ag M<sub>5</sub>N<sub>4,5</sub>N<sub>4,5</sub>) = 719.8 eV and



$\alpha$  (Ag 3d – Ag M<sub>4</sub>N<sub>4.5</sub>N<sub>4.5</sub>) = 725.6 eV, which is consistent with literature values for silver oxide (Table S1).<sup>[34]</sup>

While the room-temperature drying of the reactive silver ink on glass slides yields to highly conductive layers (*ca.* 10<sup>6</sup> S m<sup>-1</sup>),<sup>[5]</sup> the implementation of this 24 hour procedure to paper forms non-conductive brown coatings (Figure 3c). Indeed, the Walker *et al.* strategies, either performed at room-temperature for several hours or at 90 °C for several minutes, are not transposable to paper substrates due to the wetting and rapid penetration by the MOD ink (Figure 3c). The very close morphology of the scanning electron microscope (SEM) images of the pristine paper (Figure 3a) and the paper coated with the MOD ink (Figure 3b) supports that in the absence of rapid plasma sintering, the MOD ink almost fully penetrates into the porous paper substrate. In particular, the numerous 1 μm large pinholes of the paper substrate are clearly observed on the MOD ink coated sample (Figure 3b). On the other hand, the immediate (*ca.* 800 μs) plasma sintering of the inkjet printed silver MOD ink led to the formation of a silvery metallic coating (*ca.* 2 μm thickness) with a conductivity of 3.8 × 10<sup>6</sup> S m<sup>-1</sup> on paper. This value is one order of magnitude lower than the bulk silver conductivity reported by Walker *et al.* for a 15 minutes sintering at 90 °C of the same ink on glass. This surpasses by far the conductivity reported for all other room-temperature and atmospheric-pressure deposition routes toward silver coatings on paper.

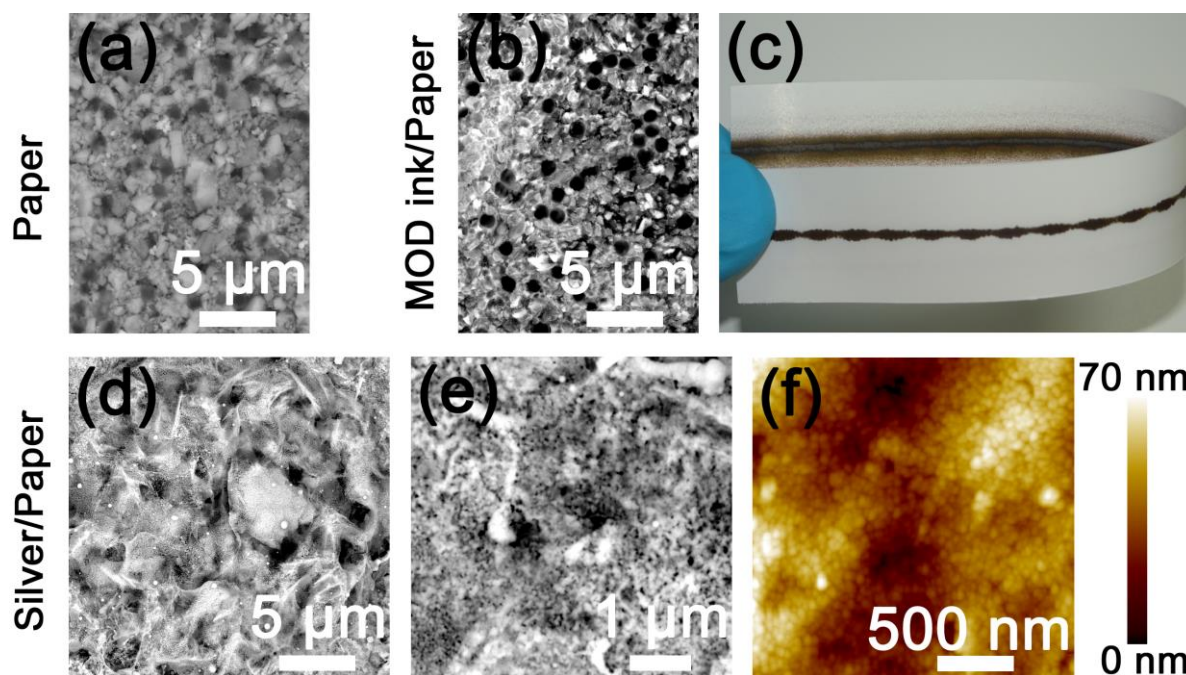


**Figure 3.** Paper wetting and conductivity. SEM images of a) pristine paper and b) MOD ink-coated paper dried at room-temperature. c) Front and back-side large area inkjet printed MOD ink deposited on paper and dried at room-temperature in air. d) and e) are the low and high magnification SEM images of the plasma-assisted inkjet printed silver on paper, respectively. f) AFM image of the plasma-assisted inkjet printed silver on paper.

In contrast to the previous SEM observations made of the MOD ink coated paper, the plasma-assisted inkjet printed silver layer appears to provide a fair coverage of the paper substrate (Figure 3d). Atomic force microscopy (AFM) and high magnification SEM reveal *ca.* 50 nm particles that form a three-dimensionally interconnected pathway (Figure 3e & f). Nevertheless, both large (Figure 3d) and small voids (Figure 3e) are also observed all across the surface. Since the complete conversion from MOD ink to silver is carried out under the plasma, the presence of voids is likely the limiting factor in regards to achieving bulk silver conductivity. The formation of small pinholes (*i.e.* < 100 nm) is inherent to any material deposited where gas loss is congenital to the process.<sup>[28]</sup> Whereas the micrometre-sized porosities are presumably more likely related to the wetting of the MOD ink on the rough paper substrate. Indeed, cross-sectional (Figure 1e) and low magnification top-view SEM (Figure 3f) observations of the

plasma-assisted inkjet printed silver coating, with a roughness ( $S_a = 135$  nm) similar to the paper roughness ( $S_a = 94$  nm), show that the silver coating does not evenly cover the paper substrate. In addition, whilst microscopically no permeation of the plasma-assisted inkjet printed MOD ink and therefore resultant silver coating could be detected in the paper (Figure 1e), permeation of the MOD ink cannot be fully excluded, not least because this would influence the resistivity of the metal deposited. The adhesion of the silver lines was investigated using the scotch tape adhesion test. After a rapid pulling off at an angle close to  $180^\circ$ , the tape exhibits a light and discontinuous silver coloration alongside many white areas originating from the paper substrate. Interestingly, after 100 repetitions of the scotch tape adhesion test, during which the silver coloration on the pulled off tapes progressively extinguished, the resistance indicated by the multimeter remained unchanged (*ca.*  $8 \Omega$  across a length of approximately 12 cm). This observation suggests that only loosely connected silver particles, not contributing to the layer's conductivity, are removed during the scotch tape adhesion test. The high conductivity of the layer, *i.e.*  $3.8 \times 10^6 \text{ S m}^{-1}$ , is retained after the scotch tape adhesion test.

In order to gain a better understanding of the assets and limitations of the developed plasma-assisted inkjet printing approach, silver lines were deposited under the same condition on polyethylene naphthalate (PEN) foils, which possess excellent barrier properties. Interestingly, SEM cross-sectional observations of the silver lines printed on PEN using the same volume of MOD ink (Figure S2) is in agreement with the  $2 \mu\text{m}$  thickness measured on the paper substrate. This undoubtedly confirms the negligible permeation of the MOD ink into the paper substrate during the plasma-assisted inkjet printing process. The conductivity of the silver line on PEN was evaluated to  $3.0 \times 10^6 \text{ S m}^{-1}$ , which is lower but in concordance with the value measured on the paper substrate. Further analyses of the plasma-assisted inkjet printed lines on PEN showed deposits to be mainly constituted of silver by XPS (*ca.* 92 %) and EDX (*ca.* 98 %). XPS did highlight a discrepancy between the two substrates investigated in the present work;

two distinct regions, both consistent with metallic silver in view of the Auger MNN region (Figure S3), can be observed in the XPS spectrum of the plasma-assisted inkjet printed silver on PEN (Figure S4). The disparity between the two sets of peaks is equal to the charge compensation applied by the flood gun during the XPS analysis (*i.e.* 3.0 eV) revealing that both connected and therefore conductive silver is present alongside disconnected particles of silver on the PEN substrate. A linescan across the *ca.* 1 mm wide plasma-assisted inkjet printed silver line on PEN was carried out to check the spatial evolution of the connected Ag particles / not connected Ag particles ratio on PEN. It was observed across the breadth of the line that at the peripheries the disconnected Ag particles were in abundance but in the centre of the sample connected Ag particles make up the majority of the silver in the sample (*i.e.* 82 %) (Figure S5). Such an observation is not surprising as the rather low surface energy of the PEN substrate (WCA = 85°) is not expected to favour its uniform wetting by the MOD ink, leading to the formation of a loosely-packed film with conductivity one-order of magnitude lower than bulk silver. If the deficient wetting of the MOD ink on paper may find its origin more on the surface roughness of the paper substrate rather than on its surface chemistry, it still results in a reduced conductivity (*i.e.*  $3.75 \cdot 10^6 \text{ S m}^{-1}$ ) of the plasma-assisted inkjet printed silver on paper compared to bulk silver. In both cases, increasing the number of inkjet printing and plasma sintering cycles should substantially improve the conductivity. In other words, the process can be adjusted for the desired output resistivity on paper and plastic substrates for flexible and lightweight electronic applications.

In conclusion, the plasma-assisted inkjet printing of a silver MOD ink has yielded the formation of highly conductive (*i.e.*  $3.8 \cdot 10^6 \text{ S m}^{-1}$ ) silver on paper, overcoming the wetting issues often encountered on porous substrates. Moving away from thermal sintering, plasma sintering has been shown to be an effective conversion tool to produce conductive metal tracks at room-temperature and atmospheric-pressure. Therefore, the proposed approach is thus particularly

suitable for the coating of porous and temperature sensitive substrates such as paper. Indeed, paper's physical and mechanical properties alter well below its autoignition temperature (*ca.* 200 °C), and this method removes the need for complex strategies such as hot-pressure sintering for example (which have been developed to form conductive silver patterns on paper).<sup>[35]</sup> Our plasma-assisted inkjet printing approach, yielding the formation of 2 μm thick silver on paper in less than 10 minutes, considerably shortens the time required to form highly conductive silver on paper.<sup>[36]</sup> As a consequence, the developed strategy may aid in the realization of low-cost flexible and paper-based electronic devices, including high frequency devices. In addition, the developed plasma-assisted inkjet printing approach is assuredly not specific to paper substrates and can be easily be implemented on other materials substrates, where it may be coupled to conventional sintering methods to reduce both the sintering time and temperature required to convert MOD inks to metal.

### Experimental Section

*Plasma-assisted inkjet printing of highly conductive silver on paper:* Highly conductive silver lines were deposited on paper in semi-industrial atmospheric-pressure dielectric barrier discharge reactor composed of two high voltage electrodes covered by a dielectric material (*i.e.* alumina) and a moving stage on which was placed the paper substrate (*i.e.* HP soft gloss laser paper). In the first step, the silver MOD ink,  $[\text{Ag}(\text{NH}_3)_2]^+[\text{C}_2\text{H}_3\text{O}_2]^-$ , was inkjet printed on the paper substrate using a MicroMist ultrasonic nozzle operating at 120 kHz and coupled to an air shaping system from Sono-Tek. The inkjet printing step was performed in the dynamic mode ( $10 \text{ cm s}^{-1}$ ) and *ca.*  $14 \text{ nL cm}^{-2}$  were deposited per cycle. Promptly (*ca.* 800 μs) after the inkjet printing step, the paper substrate was briefly exposed (*ca.* 2 s) to an atmospheric-pressure plasma discharge ignited in a mixture of argon and hydrogen (97.5 %-2.5 %) using a 10,000 Hz sinusoidal signal generated by a Corona generator 7010R from SOFTAL electronic GmbH.<sup>[37]</sup> The discharge gap between the high voltage electrodes and the paper sheet was 1 mm. The 2 μm

thick silver layers described in this study were prepared from 200 inkjet printing and plasma sintering cycles, corresponding to a 400 s effective time under the plasma discharge.

### Supporting Information

Supporting Information is available from the Wiley Online Library.

### Acknowledgements

The Ramsay Memorial Trust is thanked for funding C.E.K. Additionally, C.E.K. is particularly grateful to the Luxembourg National Research Fund for supporting her visiting scientist position at LIST through the PLASMID (INTER/MOBILITY/17/11595373) project. Dr. K. Baba, J.-L. Biagi and P. Grysan from LIST are acknowledged for insightful discussions and acquisition of the SEM and AFM measurements.

Received: ((will be filled in by the editorial staff))

Revised: ((will be filled in by the editorial staff))

Published online: ((will be filled in by the editorial staff))

### References

- [1] D. Tobjörk, R. Österbacka, *Adv. Mater.* **2011**, *23*, 1935.
- [2] R.-Z. Li, A. Hu, T. Zhang, K. D. Oakes, *ACS Appl. Mater. Interfaces* **2014**, *6*, 21721.
- [3] S. Magdassi, A. Kamyshny, Eds. , *Nanomaterials for 2D and 3D Printing*, Wiley-VCH, Weinheim, **2017**.
- [4] S. Wünscher, R. Abbel, J. Perelaer, U. S. Schubert, *J Mater Chem C* **2014**, *2*, 10232.
- [5] S. B. Walker, J. A. Lewis, *J. Am. Chem. Soc.* **2012**, *134*, 1419.
- [6] V. Sanchez-Romaguera, S. Wünscher, B. M. Turki, R. Abbel, S. Barbosa, D. J. Tate, D. Oyeka, J. C. Batchelor, E. A. Parker, U. S. Schubert, S. G. Yeates, *J Mater Chem C* **2015**, *3*, 2132.
- [7] K. Xiong, G. Emilsson, A. Maziz, X. Yang, L. Shao, E. W. H. Jager, A. B. Dahlin, *Adv. Mater.* **2016**, *28*, 9956.
- [8] J. S. Jur, W. J. Sweet, C. J. Oldham, G. N. Parsons, *Adv. Funct. Mater.* **2011**, *21*, 1993.
- [9] S. Wünscher, B. Seise, D. Pretzel, S. Pollok, J. Perelaer, K. Weber, J. Popp, U. S. Schubert, *Lab Chip* **2014**, *14*, 392.
- [10] Y. Li, Y. Wu, B. S. Ong, *J. Am. Chem. Soc.* **2005**, *127*, 3266.
- [11] S. Wünscher, S. Stumpf, A. Teichler, O. Pabst, J. Perelaer, E. Beckert, U. S. Schubert, *J. Mater. Chem.* **2012**, *22*, 24569.
- [12] W. M. Haynes, D. R. Lide, Eds. , *CRC Handbook of Chemistry and Physics: A Ready-Reference Book of Chemical and Physical Data*, CRC Press, Boca Raton, Fla., **2015**.
- [13] H. Wu, S. W. Chiang, W. Lin, C. Yang, Z. Li, J. Liu, X. Cui, F. Kang, C. P. Wong, *Sci. Rep.* **2015**, *4*, DOI 10.1038/srep06275.
- [14] K. Black, J. Singh, D. Mehta, S. Sung, C. J. Sutcliffe, P. R. Chalker, *Sci. Rep.* **2016**, *6*, DOI 10.1038/srep20814.
- [15] S. F. Jahn, T. Blaudeck, R. R. Baumann, A. Jakob, P. Ecorchard, T. Rüffer, H. Lang, P. Schmidt, *Chem. Mater.* **2010**, *22*, 3067.
- [16] C.-N. Chen, T.-Y. Dong, T.-C. Chang, M.-C. Chen, H.-L. Tsai, W.-S. Hwang, *J. Mater. Chem. C* **2013**, *1*, 5161.

- [17] M. Vaseem, G. McKerricher, A. Shamim, *ACS Appl. Mater. Interfaces* **2016**, *8*, 177.
- [18] A. L. Dearden, P. J. Smith, D.-Y. Shin, N. Reis, B. Derby, P. O'Brien, *Macromol. Rapid Commun.* **2005**, *26*, 315.
- [19] Y.-K. Liu, M.-T. Lee, *ACS Appl. Mater. Interfaces* **2014**, *6*, 14576.
- [20] J. J. P. Valetton, K. Hermans, C. W. M. Bastiaansen, D. J. Broer, J. Perelaer, U. S. Schubert, G. P. Crawford, P. J. Smith, *J. Mater. Chem.* **2010**, *20*, 543.
- [21] J. S. Kang, J. Ryu, H. S. Kim, H. T. Hahn, *J. Electron. Mater.* **2011**, *40*, 2268.
- [22] M. L. Allen, M. Aronniemi, T. Mattila, A. Alastalo, K. Ojanperä, M. Suhonen, H. Seppä, *Nanotechnology* **2008**, *19*, 175201.
- [23] E. T. Thostenson, T.-W. Chou, *Compos. Part Appl. Sci. Manuf.* **1999**, *30*, 1055.
- [24] J. Perelaer, R. Jani, M. Grouchko, A. Kamyshny, S. Magdassi, U. S. Schubert, *Adv. Mater.* **2012**, *24*, 3993.
- [25] M. Quesada-González, K. Baba, C. Sotelo-Vázquez, P. Choquet, C. J. Carmalt, I. P. Parkin, N. D. Boscher, *J Mater Chem A* **2017**, *5*, 10836.
- [26] N. D. Boscher, P. Choquet, D. Duday, S. Verdier, *Surf. Coat. Technol.* **2010**, *205*, 2438.
- [27] K. Baba, S. Bulou, P. Choquet, N. D. Boscher, *ACS Appl. Mater. Interfaces* **2017**, *9*, 13733.
- [28] I. Reinhold, C. E. Hendriks, R. Eckardt, J. M. Kranenburg, J. Perelaer, R. R. Baumann, U. S. Schubert, *J. Mater. Chem.* **2009**, *19*, 3384.
- [29] M. Vaseem, S.-K. Lee, J.-G. Kim, Y.-B. Hahn, *Chem. Eng. J.* **2016**, *306*, 796.
- [30] P. Dvorak, M. Talaba, A. Obrusnik, J. Kratzer, J. Dedina, *Plasma Sources Sci. Technol.* **2017**, *26*, 085002.
- [31] S. Ghosh, E. Klek, C. A. Zorman, R. M. Sankaran, *ACS Macro Lett.* **2017**, *6*, 194.
- [32] W. C. Ellis, C. R. Lewis, A. P. Openshaw, P. B. Farnsworth, *J. Am. Soc. Mass Spectrom.* **2016**, *27*, 1539.
- [33] N. Pauly, F. Yubero, S. Tougaard, *Appl. Surf. Sci.* **2016**, *383*, 317.
- [34] A. M. Ferraria, A. P. Carapeto, A. M. Botelho do Rego, *Vacuum* **2012**, *86*, 1988.
- [35] F. Wang, P. Mao, H. He, *Sci. Rep.* **2016**, *6*, 21398.
- [36] R. Singh, E. Singh, H. S. Nalwa, *RSC Adv.* **2017**, *7*, 48597.
- [37] N. D. Boscher, D. Duday, S. Verdier, P. Choquet, *ACS Appl. Mater. Interfaces* **2013**, *5*, 1053.

**The plasma-assisted inkjet printing of metal-organic decomposition (MOD) inks** is demonstrated to provide an easily up-scalable method towards the deposition of highly conductive silver features on paper. Atmospheric plasma sintering provide a fast and effective alternative to thermal treatment. This high-speed, room-temperature technique allows to immediately convert the MOD inks after printing and thus overcomes wetting issues typically encountered in porous substrates.

Keywords: silver patterning, MOD inks, room-temperature sintering, inkjet printing, atmospheric plasma

C. E. Knapp,\* J.-B. Chemin, S. P. Douglas, D. Abessolo Ondo, J. Guillot, P. Choquet, N. D. Boscher\*

### Room-Temperature Plasma-Assisted Inkjet Printing of Highly Conductive Silver on Paper

